THE JOURNAL OF PHYSICAL CHEMISTRY B

ARTICLE

pubs.acs.org/JPCB

Thermal Aging of Interfacial Polymer Chains in Ethylene−Propylene−Diene Terpolymer/Aluminum Hydroxide Composites: Solid-State NMR Study

Brice Gabrielle, Cédric Lorthioir,* and Françoise Lauprêtre

Equipe "Systèmes Polymères Complexes", Institut de Chimie et des Matériaux Paris-Est (UMR 7182 CNRS/Université Paris-Est Créteil), 2-8 rue Henri Dunant, 94320 Thiais, France

ABSTRACT: The possible influence of micrometric-size filler particles on the thermo-oxidative degradation behavior of the polymer chains at polymer/filler interfaces is still an open question. In this study, a cross-linked ethylene−propylene−diene (EPDM) terpolymer filled by aluminum trihydrate (ATH) particles is investigated using ^{1}H solid-state NMR. The time evolution of the EPDM network microstructure under thermal aging at 80 °C is monitored as a function of the exposure time and compared to that of an unfilled EPDM network displaying a similar initial structure. While nearly no variations of the topology are observed on the neat EPDM network over 5 days at 80 °C, a significant amount of chain scission phenomena are evidenced in EPDM/ATH. A specific surface effect induced by ATH on the thermodegradative properties of the polymer chains located in their vicinity is thus pointed out. Close to the filler particles, a higher amount of chain scissions are detected, and the characteristic length scale related to these interfacial regions displaying a significant thermo-oxidation process is determined as a function of the aging time.

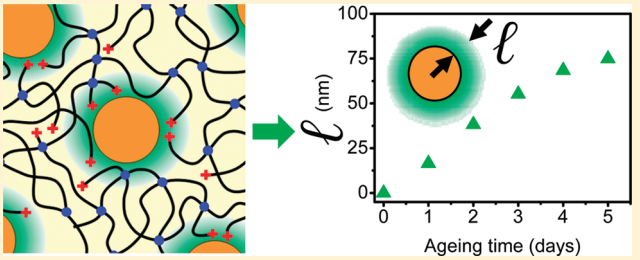

1. INTRODUCTION

In polymer-based microcomposites, the evolution of the polymer chain structure induced by thermal aging is usually assumed to be essentially the same as that which would be observed, under the same conditions, for the unfilled matrix. Indeed, in contrast to nanocomposite materials, the contact area between the filler and the polymer chains is rather low in a microcomposite, even for systems displaying a very good dispersion of the micrometric-size filler particles within the matrix. Therefore, specific influences of the filler on the thermal oxidative degradation behavior of the chains at the polymer/filler interfaces, if any, are implicitly considered to affect a negligible fraction of the polymer chains. As a result, similar evolutions of the matrix under thermal aging are expected for a composite and the corresponding unfilled polymer. The purpose of this work is to determine whether this assumption is always appropriate. To address this question from an experimental point of view, a model microcomposite, composed of a cross-linked ethylene−propylene−diene (EPDM) elastomer as the polymer matrix and aluminum trihydrate (ATH) particles as the filler component, is considered.

EPDM terpolymers are very versatile materials since their physical properties strongly depend on their composition, the copolymer microstructure, and the nature of the diene. Depending on the propylene unit content, for instance, amorphous or semicrystalline matrixes may be obtained. Besides, the unsaturation of the diene may be used to cross-link the EPDM chains through sulfur vulcanization or peroxide cure, for instance. In addition to this variety of solid-state organizations that can be obtained, other intrinsic properties of EPDM chains such as oxygen or heat resistance as well as very good electric properties, for example, justify that EPDM are used for a wide range of applications.

In particular, because of their excellent electric insulating performances, EPDM terpolymers are well-suited for wire insulation and sheathing of cables involved in nuclear power plants or in low to intermediate voltage applications. In such cases, a flame-retardant compound is usually incorporated to enhance the rather low ignition resistance of the polymer matrix. Several kinds of flame retardants are usually considered, such as halogenated molecules or metal hydroxides, for instance. In recent years, halogen-free flame retardants have been more and more widespread in the cable industry, mainly for environmental reasons. Compounds such as ATH or magnesium hydroxide offer a good alternative since they do not give rise to toxic or corrosive substances when burning. One of the drawbacks when using metal hydroxides as flame retardants such as ATH or magnesium hydroxide is the high amount that has to be incorporated within the polymer matrix, 60 wt % typically, to achieve the required efficiency of flame retardancy.

Due to their saturated backbone, EPDM elastomers are rather resistant to degradation by heat, in comparison to other conventional rubbers such as polybutadiene or polyisoprene, for instance. The thermodegradative properties of EPDM under an oxygen atmosphere have been thoroughly investigated in the past, with a detailed description of the variation of its chemical

Received: July 25, 2011
Revised: September 23, 2011
Published: September 26, 2011

structure during aging, on the basis of FTIR spectroscopy, gaseous derivatization reactions, and also, to less extent, ^{13}C solid-state NMR.[1−4] The determination of the species induced by thermo-oxidation and their quantification were carried out, thus enabling mechanisms of degradation of the EPDM chains to be proposed. From another point of view, these modifications in the chemical structure of the EPDM matrix may also induce variations in the polymer chain topology: oxidation of the EPDM chains may lead to scission phenomena, while recombination of radicals formed during thermal exposure results in chain cross-linking.[2,3] Such changes of the EPDM matrix topology are relevant to understand the evolution of its mechanical/rheological properties during thermal aging.[4,5] From an experimental point of view, the topology of EPDM networks was monitored as a function of the thermal aging time by means of swelling ratio and soluble fraction measurements as well as ^1H NMR transverse relaxation experiments.[5]

In contrast, the potential effect of filler particles on the thermo-oxidation behavior of EPDM matrixes is far less reported in the literature. Assink et al. investigated the degradation of EPDM chains exposed at 140 °C in air-circulating aging ovens by means of mechanical and ^1H NMR relaxation measurements.[5] This EPDM sample was withdrawn from a commercial O-ring containing antioxidants as well as a filler component, the nature and the characteristics of which were not indicated. The changes of the polymer matrix topology in this composite were monitored as a function of the thermal aging time, but no comparison was performed with the formulation characterized by the same composition, but without the filler component. This feature precludes the detection of a possible influence of the filler particles on the thermal degradation of the EPDM network. Another investigation by Delor-Jestin et al. was dedicated to photoaging and thermal and natural aging of formulations based on EPDM homopolymers with 5-ethylidene-2-norbornene as the diene component.[4] The chemical species resulting from the various aging conditions and the time evolution of their concentrations were determined. In the case of thermal degradation, the effect of several parameters involved in conventional formulations such as zinc oxide, antioxidant (quinolein in the present case), and carbon black was systematically probed. Interestingly, the incorporation of carbon black was found to modify the kinetics of thermal aging displayed by the cross-linked EPDM matrix since a significant increase of the induction period was detected. This behavior was interpreted as resulting from a stabilizing effect of phenolic residues located at the surface of the carbon black particles.

With this feature in mind, we have investigated the potential effect of the ATH filler particles on the thermal aging of the EPDM network in an EPDM/ATH composite. A high filler loading, 60 wt % ATH, namely, was considered to mimic the formulations typically used in the wire or cable industry. In contrast to carbon black, the outer surfaces of the ATH particles should not display any stabilizing organic residue. Moreover, the specific surface area of ATH is rather low since it usually ranges between 2 and 12 $m^2 \cdot g^{-1}$, and therefore, one could expect the thermal aging behavior of the EPDM network to be identical in the EPDM/ATH composite and in the unfilled sample.

In this work, the variation of the topology of the ATH-filled EPDM network will be monitored during thermal exposure at 80 °C. For this purpose, ^1H NMR transverse relaxation signal measurements will be combined with ^1H double-quantum buildup experiments to characterize the network structure and its time evolution. The $T_2(^1H)$ relaxation signals lead to a quantification and a description of the level of molecular mobility related to the dangling chain ends of the network and the sol fraction. This type of NMR experiment has been successfully used previously to obtain a precise structure of unfilled and filled EPDM networks, before any thermal aging.[6−8] From another point of view, the density of topological constraints—cross-links or chain entanglements—in the EPDM network was probed by monitoring the motionally averaged $^1H-^1H$ dipolar couplings related to the protons of the chain portions experiencing such constraints at both extremities. These dipolar couplings were derived, experimentally, from the analysis of ^1H double-quantum buildup curves. This powerful NMR approach and its application to the study of the polymer network structure were developed quite recently.[9−11] These ^1H double-quantum-based experiments were also successfully used to probe the structure changes of silicone elastomers induced by γ-irradiation or thermal aging.[12−14] By combining ^1H NMR T_2 relaxation measurements and ^1H double-quantum buildup experiments, the variation of the network topology as a function of the thermal aging time will be determined for an EPDM network with 60 wt % ATH and compared to the results obtained on the unfilled system. If a different variation of the EPDM network structure during thermo-degradation is observed due to the presence of ATH particles, then this feature should be taken into account for the description of the evolution of the mechanical properties displayed by the composite.

2. EXPERIMENTAL SECTION

2.1. Materials. The composite sample investigated in this work corresponds to an EPDM matrix filled by ATH filler particles. The EPDM copolymer, based on 5-ethylene -2-norbornene as the diene component, was supplied by Dow Chemical (Nordel IP NDR 3722P). This terpolymer, composed of 78.4 mol % ethylene, 21.5 mol % propylene, and 0.1 mol % 5-ethylene-2-norbornene, is a semicrystalline matrix, with a glass transition temperature T_g of −44 °C and a melting temperature T_m of about 48 °C. Aluminum trihydrate (Apyral 40 CD from Nabaltec) was obtained through the Bayer process. The average size of these particles is close to 1.3 μm, with a rather broad size distribution ranging from 0.4 to 4.0 μm. Their specific surface amounts to about 3.5 $m^2 \cdot g^{-1}$. The filler content of the composite material considered in this study was set to 150 phr (i.e., 60 wt %), corresponding to a volume fraction of 36%.

The samples were kindly provided by Dr. Laurent Chazeau (MATEIS, INSA-Lyon, Lyon, France). Their process conditions are described in detail in ref 15, and only the features that are relevant for the present work will be recalled here. The EPDM matrix is introduced in an internal mixer, and after 2 min of mixing, ATH particles are added, while 3 phr of the cross-linking agent, dicumyl peroxide (DCP), is incorporated 5 min later. Mixing of the blend is performed during an additional 10 min to get a homogeneous dispersion of the cross-linking agent. The mixer temperature is maintained at 80 °C to limit any cross-linking reaction at this stage. In a second step, the ingredients are mixed within an external mixer at 80 °C for 10 min to enhance the filler dispersion. Lastly, cross-linking of the EPDM matrix was performed through compression molding at 170 °C for 10 min, using 1 mm press plates. For the sake of comparison, an unfilled EPDM network was prepared using the same process conditions. In the following, the different samples considered in this

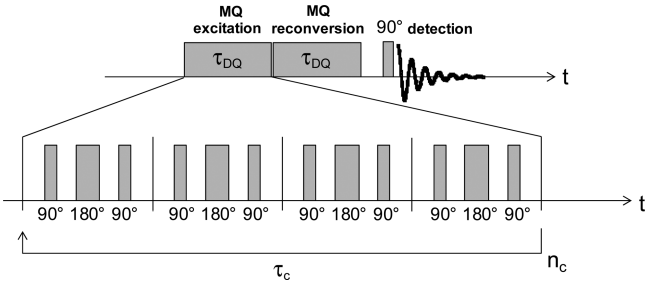

Figure 1. Schematic representation of the ^{1}H double-quantum experiment used in this work. The excitation period corresponds to a multiple integer n_c of the cycle time τ_c. The duration of the reconversion step is also equal to τ_{DQ}.

work will be denoted as "EPDM−DCP" (unfilled network) and "EPDM−DCP−ATH" (filled network).

After preparation, the EPDM matrix in EPDM−DCP and EPDM−DCP−ATH is still semicrystalline, with a melting peak ending at 59−60 °C for both materials.

2.2. Thermal Aging. The effect of thermal aging on the samples was monitored through ^{1}H NMR spectroscopy. For this aim, for each kind of materials (EPDM−DCP and EPDM−DCP−ATH), NMR experiments were carried out on the same sample part, under identical experimental conditions, after various exposure times at 80 °C under an oxidative atmosphere. The total aging time was varied from 1 to 5 days. Thermo-oxidation was performed within the NMR probe. The sample geometry (four stacked disks, each with a diameter of 4 mm and a thickness of 1 mm) was similar from one material to the other, ensuring identical thermal aging conditions within the NMR probe.

2.3. NMR Experiments. ^{1}H NMR experiments were performed on a Bruker Avance 300 NMR spectrometer operating at a ^{1}H Larmor frequency of 300.1 MHz, equipped with a 5 mm inverse ^{1}H/^{13}C-selective probe. The length of the ^{1}H 90° pulse was 7.35 μs, and the recycle delay was set to 5 s, according to the T_1(^{1}H) relaxation time of the studied samples. The temperature of the probe was calibrated between 25 and 120 °C, using the ^{1}H chemical shift measured on the methylene protons of ethylene glycol. During the NMR experiments and the thermal aging steps, the probe temperature was regulated with a stability equal to ±0.1 °C and the thermal gradient over the sample was estimated to be smaller than 0.4 °C.

2.3.1. ^{1}H Transverse Relaxation Measurements. The decay of the ^{1}H transverse magnetization was determined using the Hahn-echo pulse sequence, [90°−τ−180°−(acquisition)], as well as the solid-echo pulse sequence, [90°−τ−90°−(acquisition)]. The amplitude of the Hahn echo was monitored as a function of 2τ, for typical τ values between 0.1 and 15.0 ms. This pulse sequence enables the magnetization decay related to the NMR magnetic field inhomogeneities as well as the chemical shift dispersion to be refocused. For the solid-echo experiments, the delay τ was fixed to 12 μs and the ^{1}H transverse relaxation signal was recorded starting from the echo maximum, thus allowing the description of the initial part of the free induction decay.

2.3.2. ^{1}H Double-Quantum Experiments. ^{1}H double-quantum (DQ) experiments were performed under static conditions, using the pulse sequence initially proposed by Pines and Baum[16] and later improved by Saalwächter.[10,17] This sequence contains two periods characterized by a time τ_{DQ}, as indicated in Figure 1. The first one is aimed at exciting double-quantum coherences, while the second one leads to their reconversion into longitudinal magnetization. The corresponding signal can be read out following the last 90° pulse of the sequence, applied after a z-filter. The variation of the amplitude of the ^{1}H DQ signal as a function of τ_{DQ} leads to the buildup curve, $S_{DQ}(\tau_{DQ})$.

The determination of ^{1}H homonuclear dipolar couplings from the ^{1}H DQ buildup curve requires removing the relaxation effects involved under the pulse sequence depicted in Figure 1 on the amplitude of the ^{1}H DQ signal. In polymer networks, this may be achieved by considering the normalized DQ intensity, $I_{DQ}(\tau_{DQ})$, defined as the ratio between $S_{DQ}(\tau_{DQ})$ and the sum of $S_{DQ}(\tau_{DQ})$ and a reference signal, $S_{ref}(\tau_{DQ})$, which corresponds to the amplitude of the ^{1}H magnetization that did not evolve into $(4n + 2)$-quantum coherences. Experimentally, $S_{ref}(\tau_{DQ})$ is recorded through the same pulse sequence as that used to record $S_{DQ}(\tau_{DQ})$, only changing the receiver phase by a phase angle of 180°. Lastly, if protons that do not display ^{1}H−^{1}H dipolar couplings occur in the samples under consideration, their contribution should be removed from $S_{ref}(\tau_{DQ})$, before the normalization of the ^{1}H DQ signal, $S_{DQ}(\tau_{DQ})$. In the case of polymer networks, such contributions may arise from the occurrence of dangling chain ends or sol components.

The dependence of the normalized DQ intensity on the ^{1}H DQ excitation time, $I_{DQ}(\tau_{DQ})$, is recorded with a fixed cycle time, τ_c. The time τ_{DQ} is varied by incrementing the number n_c of cycles involved in the excitation period of the pulse sequence depicted in Figure 1. The z-filter was set to 4 μs. The excitation time values were rescaled by the factor $a = 1 - 12\tau_p/\tau_c$, τ_p standing for the ^{1}H 90° pulse length, to take into account the effect of the finite 90° and 180° pulse lengths.[17]

Complementary ^{1}H DQ measurements were performed using the five-pulse sequence, [90°−τ_{DQ}−90°−t_1−90°−τ_{DQ}−90°−t_z−(acquisition)].[18] For these experiments, both the evolution time t_1 and z-filter delay were set to 10 μs.

3. RESULTS

3.1. Unfilled EPDM Network before Thermal Aging. After peroxide cure of the EPDM homopolymers, the EPDM−DCP network still displays a semicrystalline organization. At room temperature, the protons of the crystalline regions would induce a specific component in the ^{1}H transverse relaxation signal, characterized by a decay occurring over 20 μs typically.[19] Such a fast relaxing component cannot be detected using the Hahn-echo experiment. However, the occurrence of crystallites within EPDM−DCP should also influence the segmental mobility in the amorphous phase and, thus, the ^{1}H relaxation signal determined by the Hahn-echo pulse sequence. As both the crystallinity and apparent crystallite size may vary during thermal aging,[20] the effect of the crystalline regions on the mobility of the amorphous phase may vary from one aging time to another, so that the potential differences between ^{1}H relaxation signals, induced by thermal degradation, may hardly be used to monitor the variations in the amorphous network topology. Therefore, all the NMR measurements reported in the following will be performed at 70 °C, i.e., above the end of the melting endotherm related to the network crystallites. From another point of view, we have checked that, at this temperature, the thermal aging of EPDM−DCP is not significant over the time scale of the ^{1}H NMR measurements.

The ^{1}H transverse relaxation signal obtained at 70 °C on the unaged EPDM−DCP network is depicted in Figure 2a. The

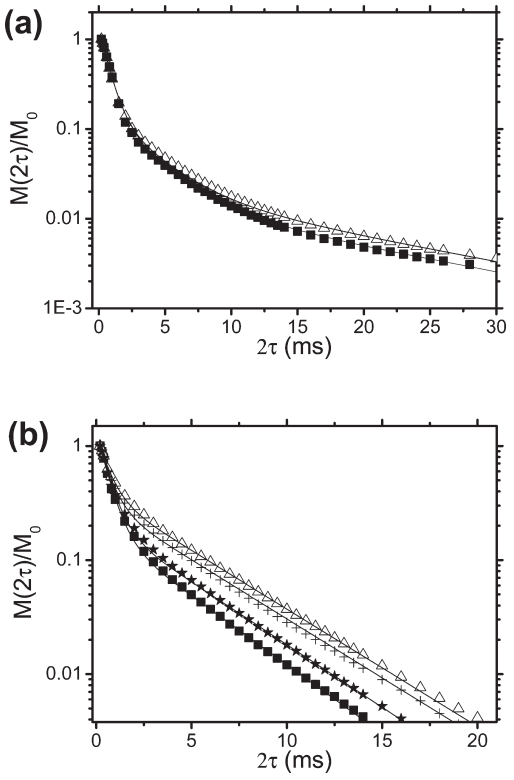

Figure 2. Evolution of the ^{1}H transverse relaxation signal as a function of the aging time, determined on both unfilled and ATH-filled EPDM networks. For EPDM−DCP (a), the results obtained before thermal aging (■) and after 5 days (△) at 80 °C are shown, while for EPDM−DCP−ATH, the measurements performed before thermal aging (■) and after 1 (★), 3 (+), and 5 (△) days at 80 °C are depicted. The measurements were performed at 70 °C. The relaxation data were normalized by M_0, the amplitude of the Hahn echo for $2\tau = 0.2$ ms. The solid lines stand for the fits of the data by the sum of three (EPDM−DCP) or two (EPDM−DCP−ATH) exponential relaxation components.

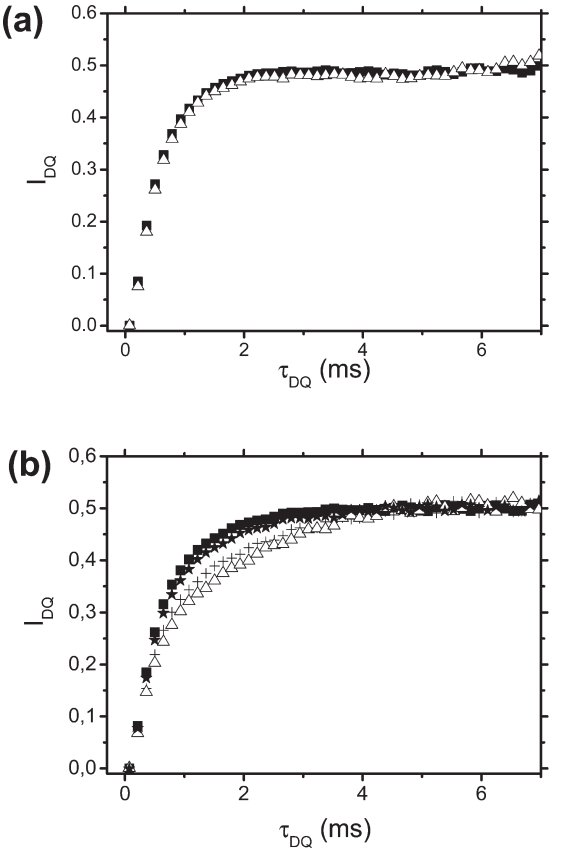

Figure 3. Variation of the normalized ^{1}H double-quantum intensity I_{DQ} with the excitation time τ_{DQ}, obtained on (a) EPDM−DCP, before thermal aging (■) and after 5 days at 80 °C (△), and (b) EPDM−DCP−ATH, before thermal aging (■) and after 1 (★), 3 (+), and 5 (△) days at 80 °C. These buildup curves were recorded at 70 °C. For each excitation time τ_{DQ}, the amplitude of the ^{1}H DQ signal, $S_{DQ}(\tau_{DQ})$, was normalized by the amplitude of the reference signal, $S_{ref}(\tau_{DQ})$, corrected by the contribution of the protons characterized by a full motional averaging of the ^{1}H dipolar couplings.

shape of the $T_2(^1\mathrm{H})$ relaxation function for entangled and/or cross-linked polymer chains such as in the case of the EPDM−DCP network is intrinsically rather complex, as evidenced by theoretical approaches aimed at describing these NMR data.[21−23] Moreover, for nonmodel polymer networks, extra complexities arising from structural heterogeneities such as the distribution of the cross-link density among the matrix make the $T_2(^1\mathrm{H})$ decay even more complex to analyze. Therefore, in the following, we will restrict our analysis of these relaxation data to a phenomenological approach. In this approximation, the relaxation signal $M(2\tau)/M_0$ may be described using three exponential components, $A_S \exp(-2\tau/T_{2S}) + A_I \exp(-2\tau/T_{2I}) + A_L \exp(-2\tau/T_{2L})$, as shown in Figure 2a. The short time decay may be assigned to the protons of chain portions constrained at both extremities, either by cross-links or by entanglements. From another point of view, after $2\tau = 17$ ms, $M(2\tau)$ may be described using a single-exponential component, characterized by a rather long $T_2(^1\mathrm{H})$ value ($T_{2L} = 17.0$ ms). This component may be assigned to mobile species, involving less than 2% of the protons. Such a slowly relaxing component may result from protons of DCP as well as additives already present in the EPDM homopolymer. Beyond these two relaxation components, an additional one is observed in Figure 2a, displaying an intermediate time decay. This component may also be described using an exponential decay. Such a contribution should result from protons displaying fast and isotropic reorientational motions, but with a lower mobility than that of the species involved in the long time decay. In particular, this component should result from chain portions constrained by a cross-link (dangling chains) or an entanglement at one side and displaying a free chain end at the other side.

The characterization of the cross-link density of EPDM−DCP may be derived from the residual ^{1}H homonuclear dipolar couplings, D_{res}. The determination of this parameter through the ^{1}H transverse relaxation signal obtained by the Hahn-echo pulse sequence may lead to erroneous values, and a method recently proposed (Figure 1), based on the ^{1}H double quantum, proved to be a reliable approach to achieve this purpose.[10] This method also enables the distribution of the D_{res} parameter to be probed and, in this way, the cross-linking inhomogeneities to be characterized.[9−11,17] Figure 3a shows the normalized ^{1}H DQ buildup curve $I_{DQ}(\tau_{DQ})$ obtained on EPDM−DCP at 70 °C.

These normalized data were obtained after subtraction of two exponential tails observed on the reference signal $S_{ref}(\tau_{DQ})$: a component corresponding to a rather small proton fraction A_C, related to a time decay T_{2C}^* of 36 ms, and a more rapidly decay-

ing component, $A_B \exp(-2\tau_{DQ}/T_{2B}^*)$, with $A_B = 8\%$ and $T_{2B}^* = 12$ ms. As proposed in ref 10, the fraction A_B was determined using the dependence of $S_{ref}(\tau_{DQ}) - S_{DQ}(\tau_{DQ}) - A_C \exp(-2\tau_{DQ}/T_{2C}^*)$ on τ_{DQ}. The normalized ^{1}H DQ intensity I_{DQ} displays an increase in the short DQ excitation time regime, and for τ_{DQ} higher than 2.2 ms, a plateau at 0.5 is observed, as expected. The experimental data cannot be satisfactorily described using the relation

$$I_{DQ}(\tau_{DQ}) = \frac{1}{2}\left[1 - \exp\left(-\frac{2}{5} D_{res}^2 \tau_{DQ}^2\right)\right] \quad (1)$$

and the best fitting line was obtained for a D_{res} value of about 380 Hz. This feature indicates that a significant distribution of the residual ^{1}H dipolar couplings, induced by spatial inhomogeneities in the repartition of the topological constraints (either cross-links or entanglements), occurs within the EPDM−DCP network. This result is consistent with the fact that the maximum observed for homogenously cross-linked networks, which results from a narrow distribution of D_{res},[11] is not observed in Figure 3a.

3.2. ATH-Filled EPDM Network before Thermal Aging. The filler content of the composite considered in this study is equal to 150 phr. The fraction of the corresponding hydroxide protons can be estimated to be 34% of the total amount of protons in EPDM−DCP−ATH. However, the ^{1}H transverse relaxation signal of neat ATH displays a fast time decay: after 20 μs, ^{1}H solid-echo experiments indicate that the amplitude of the ^{1}H transverse magnetization has reached less than 1% of that of the ^{1}H magnetization at full equilibrium. This feature results from strong ^{1}H−^{1}H dipolar couplings between the OH protons of ATH. As a result, the contribution of the ATH protons to the ^{1}H T_2 relaxation decay determined on EPDM−DCP−ATH by means of the Hahn-echo pulse sequence can be neglected. Therefore, the ^{1}H transverse relaxation signal, reported in Figure 2b, allows the topology of the EPDM network formed in the presence of the ATH filler particles to be probed.

The long $T_2(^1H)$ component detected in EPDM−DCP is not observed here, indicating that the sol fraction is smaller than that determined on EPDM−DCP by NMR, i.e., less than about 2%. As a result, the ^{1}H T_2 relaxation signal of the EPDM network in EPDM−DCP−ATH may be described phenomenologically using two exponential components, $A_S \exp(-2\tau/T_{2S}) + A_L \exp(-2\tau/T_{2L})$, as can be seen in Figure 2b: a fast decay related to the chain portions constrained by topological constraints at both extremities and the slowest decay that may be assigned to chain portions with a single free extremity. The proportion of the latter relaxation component is found to be nearly identical in both unfilled and ATH-filled EPDM networks, about 17−18%.

As for the ^{1}H T_2 measurements, the contribution of the ATH hydroxide protons should be considered in the analysis of the ^{1}H double-quantum experiments carried out on EPDM−DCP−ATH. The transverse relaxation of the ^{1}H magnetization obtained on neat ATH indicates that the OH protons of the filler particles are involved in strong ^{1}H−^{1}H dipolar couplings. Thus, the ^{1}H DQ buildup curve of neat ATH, depicted in Figure 4, was recorded using the five-pulse sequence[18] since it allows the amplitude of the ^{1}H double-quantum signal to be monitored for short DQ excitation times τ_{DQ}.

In the present case, a rather sharp maximum of the ^{1}H DQ signal, S_{DQ}, is obtained for $\tau_{DQ} = 12$ μs, corresponding to a ^{1}H dipolar coupling constant of a few tens of kilohertz. This result is consistent with the ^{1}H T_2 relaxation data obtained on neat ATH, using the solid-echo pulse sequence. The same ^{1}H buildup curve was obtained on EPDM−DCP−ATH, using the five-pulse sequence (see Figure 4). The shortest ^{1}H DQ excitation time that could be achieved using the NMR experiment depicted in Figure 1, under our instrumental conditions, is much higher than the time corresponding to the maximum of the ^{1}H DQ buildup curve displayed by the ATH hydroxide protons. This feature indicates that, in the case of EPDM−DCP−ATH, the ^{1}H DQ signal S_{DQ}, obtained through the pulse sequence represented in Figure 1, does not include any contribution from the ATH protons and can be analyzed as resulting exclusively from the residual ^{1}H dipolar couplings related to the constrained EPDM network chains.

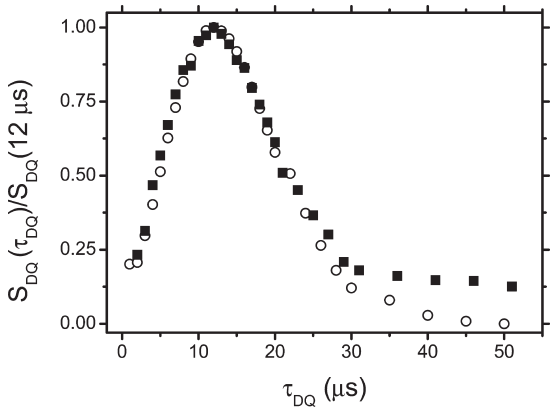

Figure 4. ^{1}H DQ buildup curve recorded on neat ATH (○) and EPDM−DCP−ATH before thermal aging (■), using the five-pulse sequence. The measurements were performed at 80 °C, with an evolution time t_1 of 10 μs and a z-filter delay fixed to 10 μs. The ^{1}H DQ values, S_{DQ}, were normalized by the highest amplitude of the DQ signal, achieved for an excitation time τ_{DQ} of 12 μs for both samples.

The ^{1}H DQ buildup curve obtained on EPDM−DCP−ATH, reported in Figure 3b, is nearly identical to that determined on EPDM−DCP. This result suggests that the distribution of the topological constraints is the same for the unfilled and the ATH-filled EPDM network. This feature is consistent with the low specific surface of ATH: the cross-linking reaction of the EPDM chains within EPDM−DCP−ATH is expected to display essentially the same characteristics as the same reaction carried out on the bulk EPDM homopolymer. As the cross-linking time used to prepare both EPDM−DCP and EPDM−DCP−ATH samples is the same (10 min at 170 °C), a similar network topology is observed. At this stage, it is worth remarking that these results, derived from NMR measurements, are in agreement with the data obtained by Planes et al. on the same samples,[15] using swelling experiments performed in xylene, after exposure to ammonia vapors. As detailed in ref 15, such a treatment based on ammonia enables the influence of the ATH particles on the value of the swelling ratio of the EPDM network in the EPDM−DCP−ATH composite to be limited. Under these experimental conditions and taking into account the volume of the filler component in the ATH-filled network, identical swelling ratios were determined for EPDM−DCP and EPDM−DCP−ATH ,while no sol fraction was detected in both networks, within the experimental accuracy.

3.3. Effect of Thermal Aging on EPDM−DCP. ^{1}H T_2 relaxation time measurements carried out on the EPDM−DCP network, aged at 80 °C for 5 days, are reported in Figure 2a and

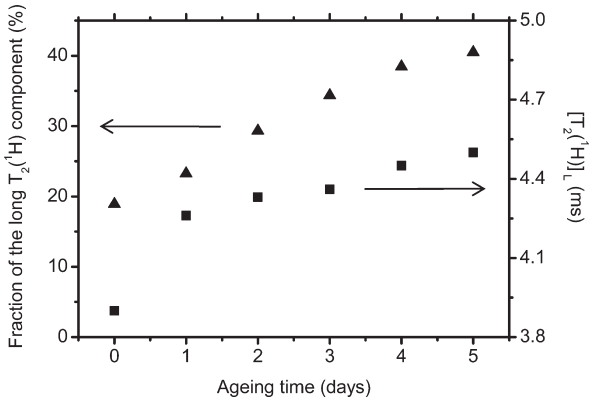

Figure 5. Effect of the thermal aging duration at 80 °C on the relaxation time $[T_2(^1H)]_L$ (■) and the fraction of protons (▲) related to the longest $T_2(^1H)$ relaxation component determined on EPDM−DCP−ATH. The ^1H transverse magnetization decays were measured at 70 °C.

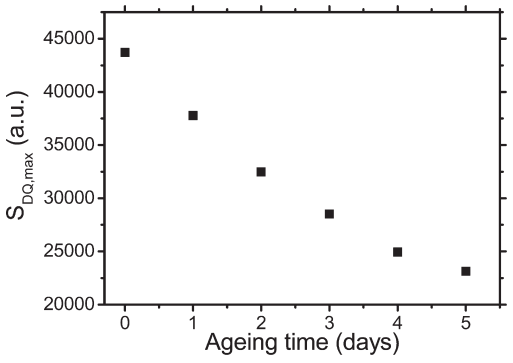

Figure 6. Dependence of the maximum value $S_{DQ,max}$ of the ^1H double-quantum signal $S_{DQ}(\tau_{DQ})$ on the thermal aging time at 80 °C, obtained for the EPDM−DCP−ATH network.

compared to the data obtained on the same sample, before thermal degradation. No significant variation of the ^1H relaxation signal occurs over this time scale. Only a slight increase of the fraction of mobile species, related to both intermediate and long time decays, is detected. This feature may be related to a weak amount of chain scission processes, leading to a slight increase of the proportion of chain portions displaying a free chain extremity, but constrained at the other end by a chemical cross-link or an entanglement. Scissions may also lead to short chains which diffuse within the network and should contribute to the longest $T_2(^1H)$ decay observed in Figure 2a.

Moreover, as far as the elastically active chains are concerned, no significant evolution of the ^1H DQ buildup curve, $I(\tau_{DQ})$, is detected over 5 days at 80 °C, as shown in Figure 3a. This result indicates that the distribution of topological constraints within the EPDM network is not affected by exposure at 80 °C over this time scale. In particular, additional cross-links would induce an extension of the distribution of residual ^1H dipolar couplings D_{res} toward high values and, thus, a faster initial rate of the corresponding ^1H DQ buildup curve. This trend is not observed in Figure 3a within the experimental accuracy, implying that thermal aging over 5 days does not lead to the formation of a significant amount of cross-links.

3.4. Effect of Thermal Aging on EPDM−DCP−ATH. Figure 2b depicts the ^1H T_2 relaxation signal recorded on the composite EPDM−DCP−ATH after various aging times at 80 °C. For exposures ranging between 1 and 5 days, the ^1H transverse relaxation function can still be described using two components, as for the unaged sample. The dependence of the proton fraction related to the longest T_2 decay as well as the corresponding relaxation time $[T_2(^1H)]_L$ on the thermal aging time is shown in Figure 5.

In contrast to the unfilled EPDM−DCP, a significant effect of exposure at 80 °C is detected as soon as ATH filler particles are present within the EPDM network. After 5 days at 80 °C, the percentage of EPDM protons involved in the long T_2 decay amounts to 40%, while its initial value, before thermal aging, was estimated to be about 19%. Besides, a slight but continuous increase of the long $T_2(^1H)$ value is also detected, as illustrated in Figure 5. The slowly relaxing component of the ^1H transverse magnetization was previously assigned to chain portions with a free extremity, the other one being either cross-linked or entangled. The experimental features observed in Figure 2b indicate that thermal aging at 80 °C induces a significant increase of chain scissions within the EPDM network of EPDM−DCP−ATH, at least up to 5 days. As the network chains undergo more and more scission phenomena, the reorientational motions of the chain portions with one free end are less and less constrained, thus accounting for their increasing level of segmental mobility evidenced by the increase of the long $T_2(^1H)$ value with the aging time (Figure 5). At this stage, it is worth recalling that the topology of the unaged EPDM network within EPDM−DCP−ATH, as revealed by ^1H T_2 relaxation measurements as well as ^1H DQ buildup curves, was rather close to that of EPDM−DCP. Therefore, the differences between the thermo-oxidative behavior clearly detected between EPDM−DCP−ATH and EPDM−DCP suggest a specific role played by the ATH filler particles.

Figure 6 shows the amplitude of the ^1H DQ signal S_{DQ} taken at the maximum of the $S_{DQ}(\tau_{DQ})$ curves determined on EPDM−DCP−ATH as a function of the thermal aging time. This maximum is observed for the same value of the ^1H DQ excitation time, τ_{DQ} = 0.8 ms, whatever the exposure time at 80 °C. From a qualitative point of view, a similar trend would be observed if a different τ_{DQ} value had been considered. Moreover, as the same sample was used for all the measurements, the absolute value of the $S_{DQ}(\tau_{DQ})$ maximum, determined under identical experimental conditions, may be directly compared before and during thermal degradation at 80 °C. Figure 6 suggests that, in the ATH-filled EPDM network, chain scission resulting from thermo-oxidation induces a lower and lower amount of chain portions constrained at both extremities. This result is in agreement with the ^1H T_2 measurements reported in Figure 5.

Nevertheless, after the normalization of the $S_{DQ}(\tau_{DQ})$ curves (see the Experimental Section), the $I_{DQ}(\tau_{DQ})$ variations for the different exposure times at 80 °C do not superimpose, as can be seen in Figure 3b. This feature indicates that, in addition to the decrease of the amount of chain portions constrained at both extremities, a significant change in the distribution of residual ^1H dipolar couplings D_{res} related to the EPDM network occurs during thermal aging of the composite. Such a behavior was not observed on the unfilled EPDM−DCP network, under the same aging conditions. Figure 3b shows that the overall growth rate of the ^1H DQ buildup curves $I(\tau_{DQ})$ decreases as the exposure time at 80 °C is raised to 5 days. This feature implies that the thermo-oxidation of EPDM−DCP−ATH results in an extension of the distribution of D_{res} toward the low ^1H dipolar coupling values.

Besides, the relative contribution of this additional component of the distribution $P(D_{res})$ increases with the thermal aging time. In other words, after a few days at 80 °C, a significant amount of EPDM chain portions experiencing weaker topological constraints than those occurring in unaged EPDM−DCP−ATH are detected.

4. DISCUSSION

The effect of filler particles on the thermal aging of an elastomeric matrix is still an open question. In the case of EPDM, to the best of our knowledge, a single reference reports the influence of a filler, carbon black particles, on the oxidation properties of an EPDM network.[4] As mentioned earlier, carbon black has a positive effect since it was found to increase the induction period. In the present work, before thermal degradation, the EPDM network filled by ATH was characterized by a topology similar to that of the unfilled sample, prepared under the same experimental conditions. However, a significantly distinct behavior was detected during thermal aging at 80 °C: while nearly no differences were observed in the unfilled network over 5 days at this temperature, chain scission phenomena occurred within the ATH-filled EPDM network, leading to a continuous and significant increase of the dangling chains and/or freely diffusing species. Correspondingly, in EPDM−DCP−ATH, the amount of chain portions constrained at both extremities was found to decrease as the thermal aging time was raised to 5 days, but the highest level of local constraint within the network remained unchanged by comparison with that determined on EPDM−DCP. In contrast, in EPDM−DCP, the amount of constrained chains does not vary over 5 days at 80 °C. Therefore, in the ATH-filled EPDM network, a significantly higher number of chain scission phenomena occur, leaving a smaller and smaller amount of regions displaying the same density of topological constraints (cross-link and/or entanglements) as the network before aging. Such a behavior is not detected on the unfilled EPDM network on the same time scale, pointing out the significant role played by the ATH component in the thermal aging process of the EPDM network. Similar trends have been recently observed in nanocomposites based on polyethylene and clay platelets displaying metallic impurities[24] as well as in polypropylene containing Ziegler−Natta catalyst:[25] in both cases, these particles were found to speed the initiation of the thermal oxidation.

At first glance, it could be tempting to interpret the results obtained on EPDM−DCP−ATH on the basis of interfacial effects exclusively: the EPDM chains located in the close surroundings of the ATH particle surface should display a different variation of their topology during thermal aging at 80 °C. However, as mentioned in section 2, the characteristic size of the ATH particles considered in this work stands in the micrometer range. Even though the filler content is rather high (150 phr, corresponding to a volume fraction of about 36%), the amount of polymer chains at the interface with the ATH particles may be neglected with respect to the bulk EPDM network chains. For instance, even though an ideal dispersion of the ATH particles within the EPDM matrix had been obtained, the amount of interfacial EPDM chain portions would be lower than 1%, considering a characteristic thickness for the interfacial zones of a few nanometers. Therefore, this result suggests that the ATH filler particles affect the thermal aging behavior of the EPDM chains located in their close surroundings, while a propagating effect toward the bulk EPDM regions should be involved to account for the different behavior observed through our NMR measurements between the EPDM chains within EPDM−DCP−ATH and EPDM−DCP. At this stage, one may suspect that, due to ATH, a higher amount of chain scission phenomena occur for the chain portions in their vicinity. Peroxy radicals $POO^{\bullet}$ are formed and may abstract the most labile hydrogen atoms of surrounding EPDM comonomer units (P′H), thus giving hydroperoxides POOH and macroradicals $P'^{\bullet}$. These macroradicals should restart the chain oxidation reactions and gradually propagate from the ATH particles toward the inner part of the EPDM matrix. As a result, a higher level of chain scission phenomena than that occurring in the unfilled EPDM network is detected experimentally since it involves not only the chains located at the interfaces with ATH, but also EPDM chains at higher distances from the filler surfaces.

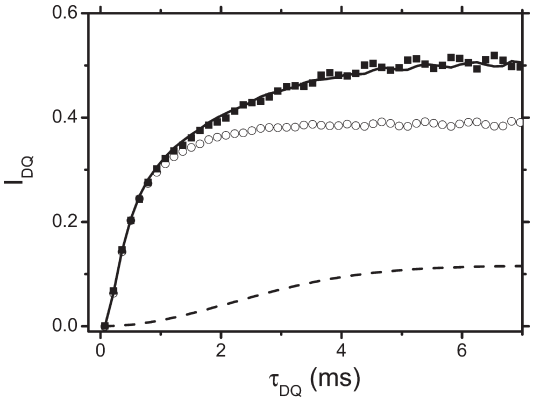

Figure 7. Description of the ^{1}H DQ buildup curve, $[I_{DQ}(\tau_{DQ})]_{aged}$, obtained on EPDM−DCP−ATH after 5 days at 80 °C (■), using two components: (1) the experimental ^{1}H DQ buildup curve of the unaged sample, $[I_{DQ}(\tau_{DQ})]_{unaged}$, rescaled to match the initial rise of $[I_{DQ}(\tau_{DQ})]_{aged}$ (○) and (2) the remaining signal that can be fitted using a single D_{res} value close to 80 Hz. This fit is reported as a dashed line and its sum with the rescaled $[I_{DQ}(\tau_{DQ})]_{unaged}$ as a solid line.

From another point of view, the ^{1}H DQ buildup curves obtained on EPDM−DCP−ATH for thermal aging times up to 5 days may be described as the linear combination of the experimental ^{1}H DQ buildup curve of unaged EPDM−DCP−ATH and an additional contribution related to a much weaker value of the residual ^{1}H dipolar couplings. This feature is illustrated in Figure 7, for an exposure time at 80 °C equal to 5 days. The relative amplitude of the additional contribution (dashed line in Figure 7) is an increasing function of the thermal aging time, as can be inferred from Figure 3b. This result may suggest that, after 5 days at 80 °C, part of the EPDM matrix in the ATH-filled network displays a topology similar to that observed before thermal aging. In other words, during thermal exposure at 80 °C, the propagation of the EPDM chain oxidation process from the ATH/matrix interfaces does not occur on the whole EPDM network, but on a characteristic length scale that will be denoted as ℓ in the following. Therefore, in the first approach, the ATH-filled EPDM−DCP network may be considered as a two-phase system during thermal degradation: one related to the EPDM regions remote from the ATH particles, characterized by a topology similar to that of the unaged composite (or, similarly, a topology similar to that of the unfilled network) and a density of topological constraints that does not vary with the thermal aging time and one assigned to the chain portions displaying a higher amount of chain scissions per unit volume, as proposed above. The chain portions corresponding to this second phase located

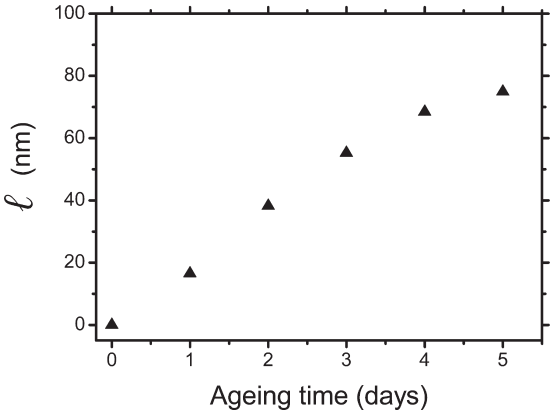

Figure 8. Evolution with the aging time at 80 °C of the characteristic length scale, ⁄, over which the thermo-oxidative behavior of the EPDM network chains is affected by the ATH filler particles.

around the ATH component should experience weaker residual ^{1}H dipolar coupling values. Indeed, the constraints on the EPDM network chains induced by trapped entanglements may be released due to the scission of one of the chains involved. In addition, the scission of a chain cross-linked at both extremities should give rise to two chain portions that may be entangled. In that case, the amplitude of the reorientational motions displayed by these chain portions, though somehow limited by the entanglements, should be much higher than that observed on the network chain before scission. For these reasons, the effective D_{res} value of the protons related to the EPDM chains within a distance ⁄ from the ATH particles is expected to be significantly lower than that determined on the unaged EPDM−DCP−ATH network. This is indeed the case, as can be seen in Figure 7.

For each thermal aging time, a rough estimation of the thickness ⁄ may be derived from the fraction A_L(aged) of the long $T_2(^1H)$ component observed on the ^{1}H transverse relaxation signal of EPDM−DCP−ATH, during exposure at 80 °C. Taking into account the initial contribution A_L(unaged) from the long $T_2(^1H)$ decay occurring in the unaged composite, ⁄ can be expressed as

$$/\approx \frac{1}{3}\frac{(1-\phi_{ATH})}{\phi_{ATH}} R[A_L(\text{aged}) - A_L(\text{unaged})] \qquad (2)$$

ϕ_{ATH} stands for the volume fraction of ATH in EPDM−DCP−ATH (ϕ_{ATH} = 36 vol %), while R denotes the average radius of the filler particles ($R \approx 650$ nm for the ATH considered in this work). Equation 2 holds in the case where ⁄ is small compared to R (⁄/$R \ll 1$). The evolution of the resulting ⁄ value during degradation at 80 °C is reported in Figure 8. This determination assumes a similar proton density for the unaged EPDM network regions and those undergoing a higher amount of chain scissions, even though thermo-oxidation results in some modifications of the chemical structure of the EPDM chains and may therefore affect the proton distribution within the polymer matrix. A cruder assumption underlying the estimation of the thickness ⁄ concerns the dispersion of the ATH particles within the EPDM network, supposed to be ideal. The dispersion of ATH in the EPDM−DCP−ATH sample, characterized by Planes et al. using scanning electron microscopy,[15] was found to be good. Nevertheless, due to the deviations with respect to an ideal dispersion, the values ⁄ reported in Figure 8 should be considered as lower limit values.

At this stage, it may be worth reminding that the chemical groups induced by the thermo-oxidation of the EPDM matrix mainly correspond to alcohols as well as ketones, carboxylic acids, and hydroperoxides.[2−4] These polar entities may display attractive interactions with the hydroxide groups located at the surface of the ATH particles. As a result, the chain portions in the vicinity of the filler should experience additional topological constraints, and even though the thermal degradation of the EPDM matrix followed the very same behavior in EPDM−DCP and EPDM−DCP−ATH, these interacting chain units in EPDM−DCP−ATH would give rise to a ^{1}H DQ signal that would not be observed in the EPDM−DCP network. In particular, the chain portions displaying a free end, resulting from scission mechanisms, and constrained by a chemical cross-link or an entanglement at the other end may interact with the surface of the ATH particles. At first glance, such adsorption phenomena could account for the additional contribution detected on the ^{1}H DQ buildup curve of EPDM−DCP−ATH during the exposure at 80 °C (dashed line in Figure 7). However, such an interpretation may be discarded since, again, the interfacial area between ATH and EPDM is rather limited in EPDM−DCP−ATH so that the attractive interactions with the filler OH groups cannot account for the significant variations observed through the ^{1}H DQ measurements performed on the protons of the EPDM network within the composite. Moreover, the adsorption of thermo-oxidized EPDM chain portions on the ATH surfaces does not allow rationalization of the significant increase in the proton fraction corresponding to the long $T_2(^1H)$ decay in the thermally aged composite material. As a result, such phenomena may occur but are not the main physical features inducing the different behaviors between the unfilled and ATH-filled EPDM−DCP network during thermal aging at 80 °C.

5. CONCLUSIONS

The time evolution of the network topology in a composite composed of EPDM and ATH under thermal aging at 80 °C was monitored through two complementary NMR approaches, ^{1}H transverse relaxation and ^{1}H double-quantum buildup measurements. An unfilled EPDM network with a structure close to that of the cross-linked chains in the composite was also investigated, as a reference system.

The comparison of the NMR data obtained on both networks during exposure at 80 °C indicates a specific effect of the ATH component on the thermo-oxidation process of the EPDM chains at the interfaces with the filler. Despite the micrometer size of the ATH particles, a propagation mechanism from the polymer/filler interfaces toward the bulk EPDM network allows the detection of this surface-induced effect. At 80 °C, the amount of chain scission phenomena in the ATH-filled EPDM network is significantly higher than that observed in the unfilled cross-linked EPDM, at least over 5 days. This feature suggests an enhancement of the scission of C−H bonds and, to less extent, C−C bonds along the EPDM chains, induced by the presence of the ATH surfaces. At this stage, experimental as well as theoretical investigations in the field of surface reactivity should help in understanding the detailed effect of ATH on the oxidation process of the EPDM chains. Moreover, this specific influence of ATH has practical implications. For instance, it should be taken into account for the estimation of the lifetime related to

EPDM/ATH composites currently involved in cables for nuclear power plants or for low to intermediate voltage applications. In this respect, the present work indicates that such a lifetime, usually determined according to mechanical criteria, cannot be predicted on the basis of the data available for unfilled EPDM networks. From a more general point of view, this study shows that assuming a similar thermal oxidative degradation behavior for a polymer matrix filled by micrometric-size particles and for the corresponding unfilled matrix is not always appropriate.

AUTHOR INFORMATION

Corresponding Author

*Phone: +33 1 49 78 13 08. Fax: +33 1 49 78 12 08. E-mail: lorthioir@icmpe.cnrs.fr.

ACKNOWLEDGMENT

This work was supported by the joint research program Composite and Polymer Ageing (COPOLA) involving EDF, LABORELEC, NEXANS France, ANDRA, CNRS, INRA, and CEA. B.G. is grateful for support in the form of a CNRS postdoctoral fellowship. C.L. gratefully acknowledges Région Ile-de-France for its participation in the purchase of the NMR spectrometer. We also thank E. Planes, L. Chazeau, and G. Vigier (MATEIS, INSA-Lyon, Lyon, France) for providing samples and for helpful discussions.

REFERENCES

(1) Palmas, P.; Le Campion, L.; Bourgeoisat, C.; Martel, L. *Polymer* **2001**, *42*, 7675–7683.
(2) Teissedre, G.; Pilichowski, J. F.; Chmela, S.; Lacoste, J. *Polym. Degrad. Stab.* **1996**, *53*, 207–215.
(3) Delor, F.; Teissedre, G.; Baba, M.; Lacoste, J. *Polym. Degrad. Stab.* **1998**, *60*, 321–331.
(4) Delor-Jestin, F.; Lacoste, J.; Barrois-Oudin, N.; Cardinet, C.; Lemaire, J. *Polym. Degrad. Stab.* **2000**, *67*, 469–477.
(5) Assink, R. A.; Gillen, K. T.; Sanderson, B. *Polymer* **2002**, *43*, 1349–1355.
(6) Litvinov, V. M. *Macromolecules* **2006**, *39*, 8727–8741.
(7) Orza, R. A.; Magusin, P. C. M. M.; Litvinov, V. M.; van Duin, M.; Michels, M. A. J. *Macromolecules* **2007**, *40*, 8999–9008.
(8) Moldovan, D.; Fechete, R.; Demco, D. E.; Culea, E.; Blümich, B.; Herrmann, V.; Heinz, M. *Macromol. Chem. Phys.* **2010**, *211*, 1579–1594.
(9) Saalwächter, K.; Herrero, B.; López-Manchado, M. A. *Macromolecules* **2005**, *38*, 9650–9660.
(10) Saalwächter, K. *Prog. Nucl. Magn. Reson. Spectrosc.* **2007**, *51*, 1–35.
(11) Valentín, J. L.; Posadas, P.; Fernández-Torres, A.; Malmierca, M. A.; González, L.; Chassé, W.; Saalwächter, K. *Macromolecules* **2010**, *43*, 4210–4222.
(12) Maxwell, R. S.; Chinn, S. C.; Solyom, D.; Cohenour, R. *Macromolecules* **2005**, *38*, 7026–7032.
(13) Giuliani, J. R.; Gjesrsing, E. L.; Chinn, S. C.; Jones, T. V.; Wilson, T. S.; Alviso, C. T.; Herberg, J. L.; Pearson, M. A.; Maxwell, R. S. *J. Phys. Chem. B* **2007**, *111*, 12977–12984.
(14) Chinn, S. C.; Alviso, C. T.; Berman, E. S. F.; Harvey, C. A.; Maxwell, R. S.; Wilson, T. S.; Cohenour, R.; Saalwächter, K.; Chassé, W. *J. Phys. Chem. B* **2010**, *114*, 9729–9736.
(15) Planes, E.; Chazeau, L.; Vigier, G.; Fournier, J.; Stevenson-Royaud, I. *Polym. Degrad. Stab.* **2010**, *95*, 1029–1038.
(16) Baum, J.; Pines, A. *J. Am. Chem. Soc.* **1986**, *108*, 7447–7454.
(17) Saalwächter, K.; Ziegler, P.; Spyckerelle, O.; Haidar, B.; Vidal, A.; Sommer, J. U. *J. Chem. Phys.* **2003**, *119*, 3468–3482.
(18) Munowitz, M.; Pines, A. *Adv. Chem. Phys.* **1987**, *66*, 1–152.
(19) Mc Brierty, V. J.; Packer, K. J. *Nuclear Magnetic Resonance in Solid Polymers*; Cambridge University Press: Cambridge, U.K., 1993.
(20) Assink, R. A.; Celina, M.; Gillen, K. T.; Clough, R. L.; Alam, T. M. *Polym. Degrad. Stab.* **2001**, *73*, 355–362.
(21) Brereton, M. G. *Macromolecules* **1990**, *23*, 1119–1131.
(22) Brereton, M. G.; Ward, I. M.; Boden, N.; Wright, P. *Macromolecules* **1991**, *24*, 2068–2074.
(23) Cohen-Addad, J. P. *Prog. Nucl. Magn. Reson. Spectrosc.* **1993**, *25*, 1.
(24) Gutiérrez, G.; Fayolle, B.; Régnier, G.; Medina, J. *Polym. Degrad. Stab.* **2010**, *95*, 1708–1715.
(25) Goss, B. G. S.; Nakatani, H.; George, G. A.; Terano, M. *Polym. Degrad. Stab.* **2003**, *82*, 119–126.